Structure, Volume *26*

Supplemental Information

Structural Basis for Auto-Inhibition of the NDR1 Kinase Domain by an Atypically Long Activation Segment

Shawn Xiong, Kristina Lorenzen, Amber L. Couzens, Catherine M. Templeton, Dushyandi Rajendran, Daniel Y.L. Mao, Yu-Chi Juang, David Chiovitti, Igor Kurinov, Sebastian Guettler, Anne-Claude Gingras, and Frank Sicheri

Supplementary Figure 1

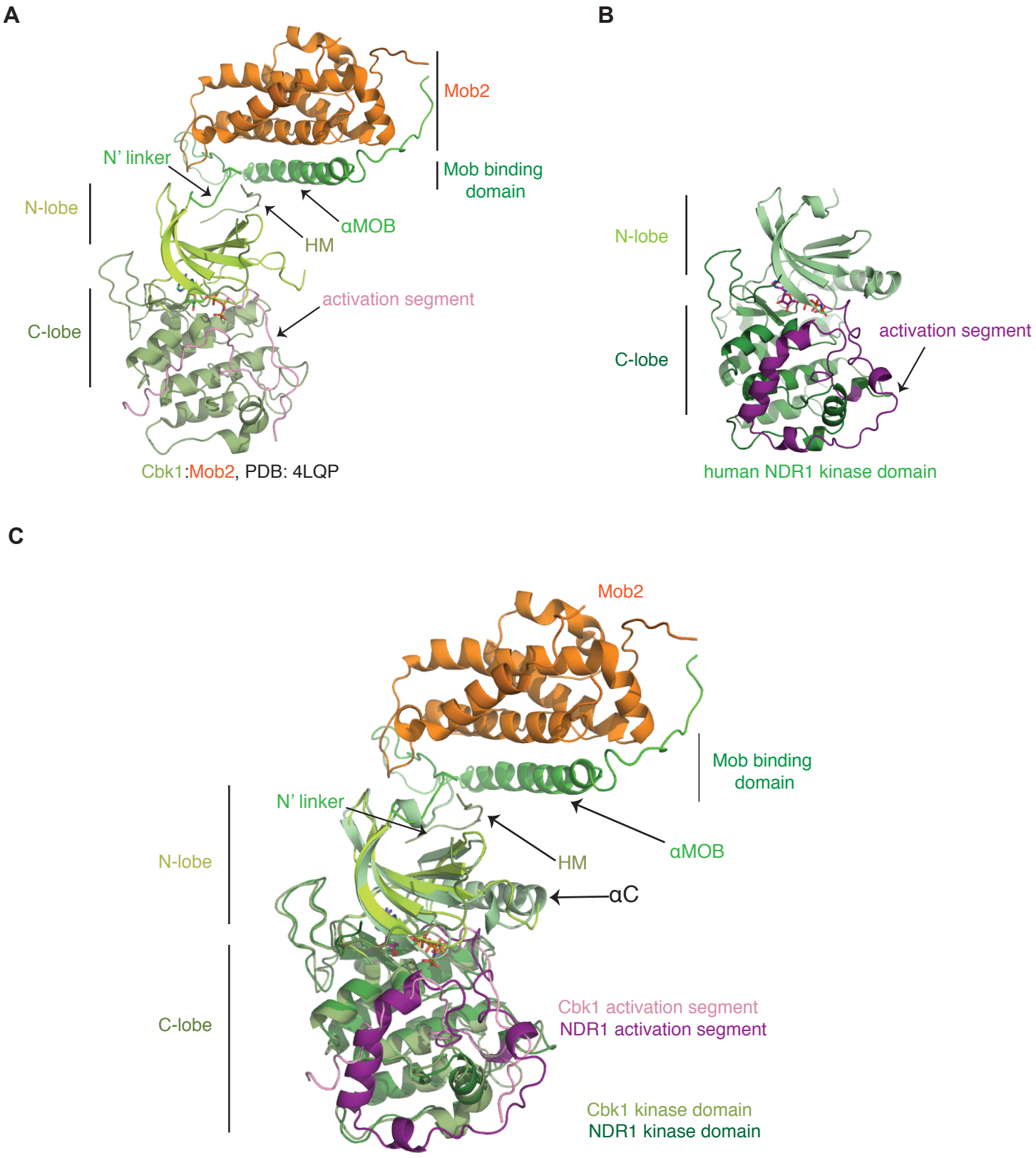

Supp. Figure 1. Structural comparison of the inactive human NDR1 kinase domain with the S. cerevisiae Cbk1-Mob2 complex. A. Crystal structure of budding yeast Cbk1^{MBD-KD} (residues 251-756) bound to Mob2 (residues 45-287) (PDB: 4LQQ; Gogl et al., 2015). B. Crystal structure of human NDR1^{KD} solved here. C. Superimposition of the yeast Cbk1-Mob2 complex and human NDR1. (Supp. Figure 1 relates to Figures 1 & 6).

Supplementary Figure 2

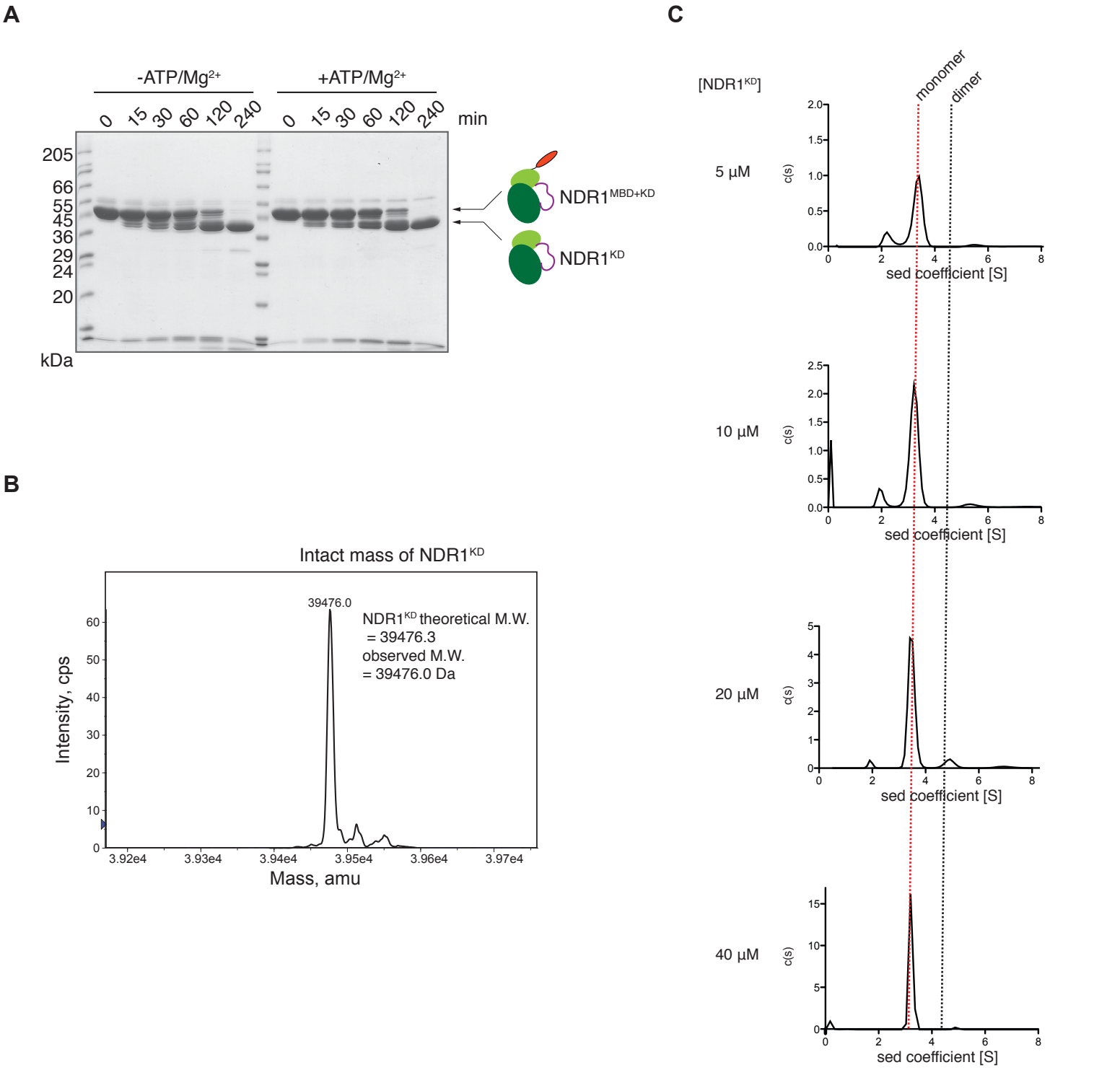

Supp. Figure 2. Biochemical and biophysical characterization of NDR1^{KD}. A. Limited proteolysis time course analysis of NDR1^{MBD-KD} by trypsin. N-terminal boundaries of the indicated protein species were determined by Edman degradation. B. Intact mass spectrum of NDR1^{KD} revealing the absence of post-translational modifications. C. Oligomer state analysis of NDR1^{KD} by analytical ultracentrifugation. Sedimentation-coefficient (S) distribution is plotted for the indicated concentrations of NDR1^{KD}. Expected positions of monomer and dimer species are shown. (Supp. Figure 2 relates to Figure 1).

Supplementary Figure 3

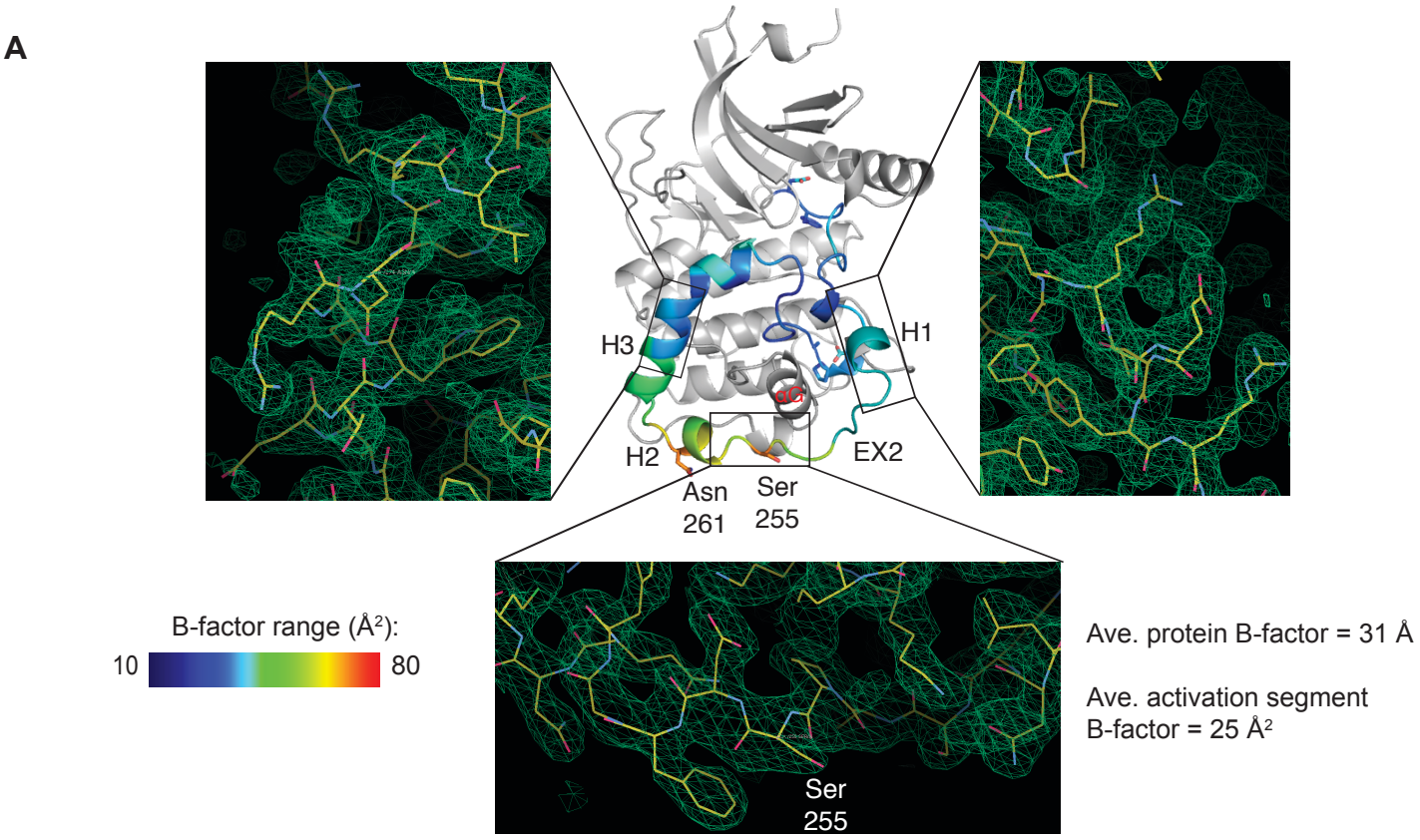

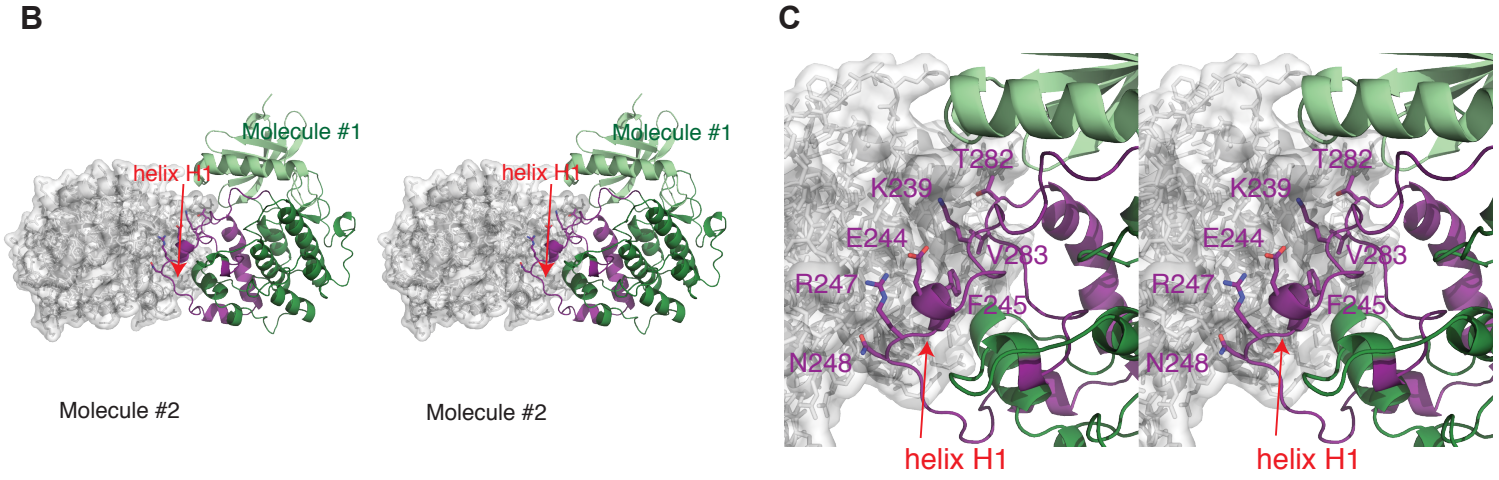

Supp. Figure 3. Structural analysis of the atypically long activation segment of NDR1. A. Ribbon representation of the kinase domain of NDR1 with the activation segment colored according to B-factor. Ser255 and Asn261 side chains with greatest B-factor are highlighted. Secondary structure elements of the activation segment are labeled. Boxed regions display representative simulated annealing composite omit electron density |2Fo-Fc| maps generated in Phenix (Afonine et al., 2012). B. Walleye stereo representation highlighting a crystal packing interaction involving the activation segment of NDR1. The contact surface is 694 Å2. For comparison, the contact surface of the activation segment with the protein kinase domain is 2740 Å2. C. Stereo zoom-in view of the contact surface highlighting contacting side chains on the activation segment. (Supp. Figure 3 relates to Figure 1).

Supplementary Figure 4

A

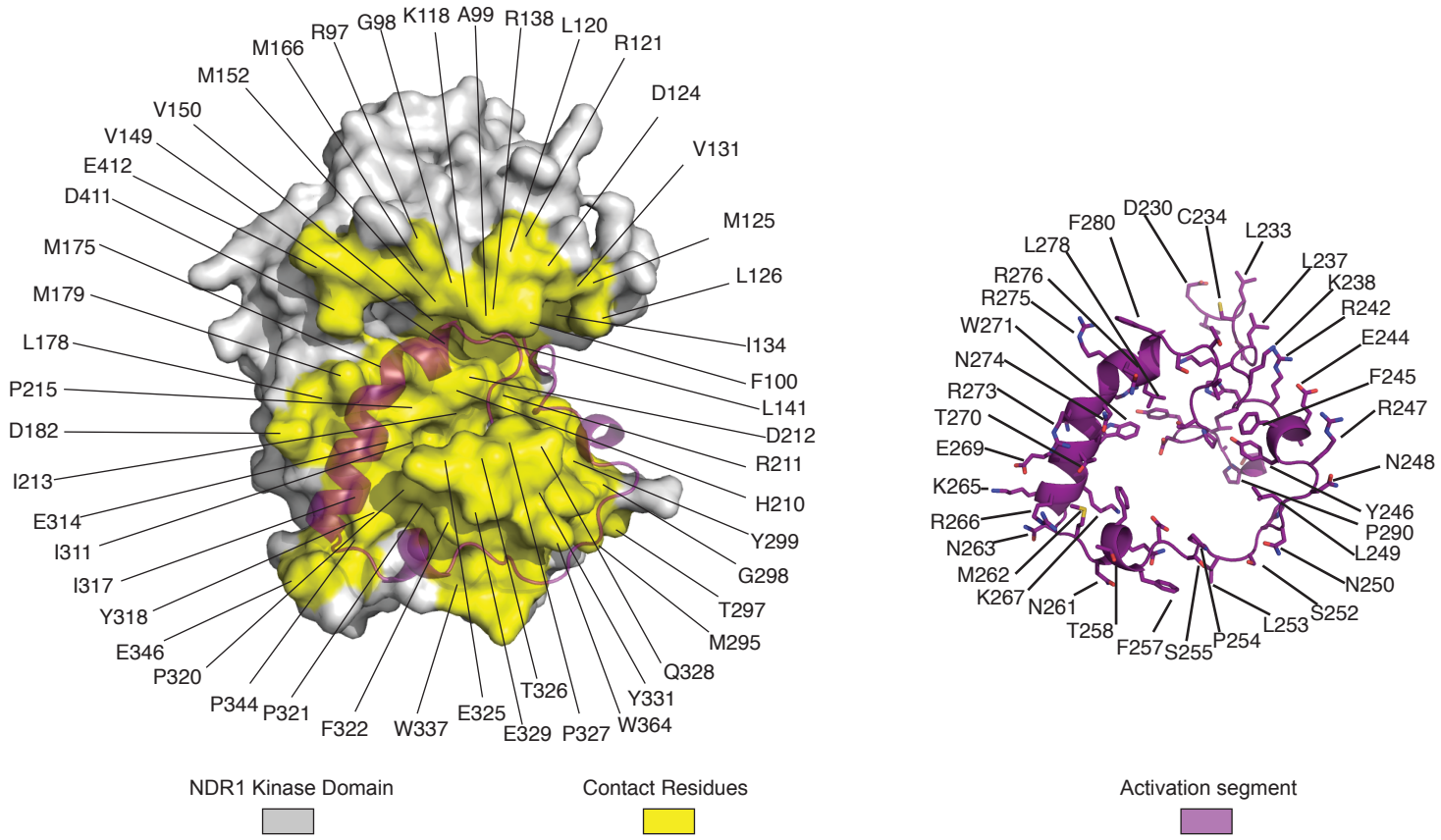

B

Hydrogen Bonds

Activation Segment	Kinase Domain
Asn250	Lys332
His251	Tyr331
Lys272	Asp181*
Lys272	Gly319*
Tyr288	Glu314
Ala290*	Val293*

* indiates backbone H-bonds

Salt Bridges

Activation Segment	Kinase Domain
Asp230	Lys118
Asp230	Arg138
Asp256	Lys333
Arg275	Asp216
Arg276	Asp411
Glu292	Arg367

Hydrophobic interactions

Activation Segment	Kinase Domain
Phe231	His210
Phe231	Leu228
Phe231	Phe208
Phe231	Ile203
Leu233	Val131
Leu233	Me125
Leu233	Ile134
Leu233	Leu162
Leu233	Leu120
Leu237	Phe100
Leu237	Leu126
Tyr246	Phe294
Tyr246	Tyr331
Leu249	Tyr331
Leu249	Lys332
Leu249	Gln328

Hydrophobic interactions

Activation Segment	Kinase Domain
Trp271	Tyr319
Trp271	Pro320
Phe280	Phe413
Pro286	Phe294
Pro286	Val334
Pro286	Pro327
Tyr288	Pro320
Tyr288	Lys214
Tyr288	Pro215
Ile289	Phe184
Ile289	Val293
Pro291	Trp306
Pro291	Trp337
Pro291	Phe322

Supp. Figure 4. Interaction of the atypically long activation segment of NDR1 with the kinase domain core. A. Left, surface representation of $NDR1^{KD}$, highlighting the residues on the kinase domain core that interact with the activation segment. Right, ribbon representation of the NDR1 activation segment, highlighting the residues that contact the kinase domain core. B. Summary of hydrogen bonds, salt bridges, and hydrophobic interactions between the NDR1 kinase domain core and the activation segment. (Supp. Figure 4 relates to Figure 1).

Supplementary Figure 5

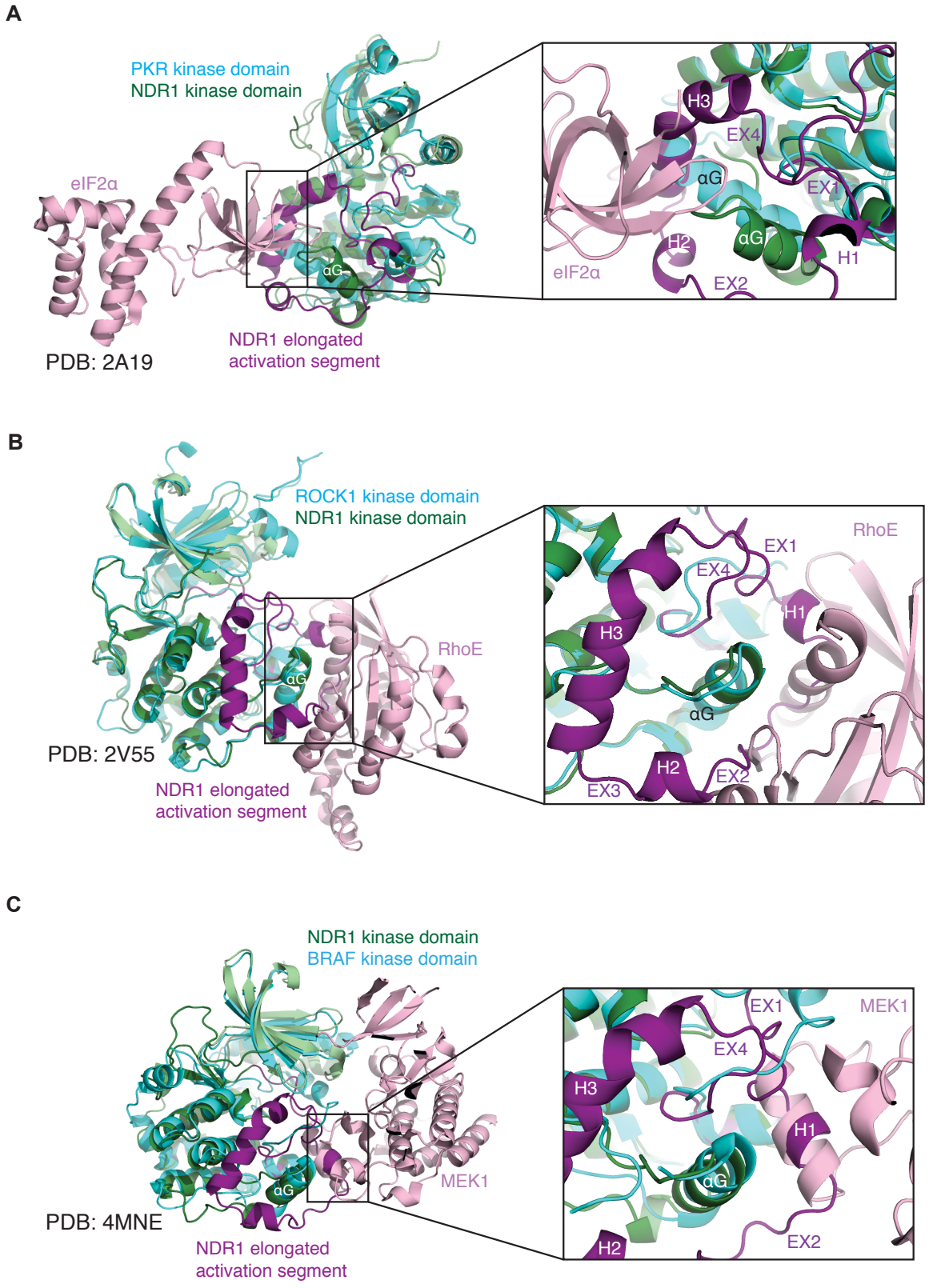

Supp. Figure 5. Comparison of the structure of NDR1^{KD} with other protein kinase domains bound to globular substrates. A. Superimposition of PKR-elF2α (PDB: 2A19; Dar et al., 2005) and NDR1^{KD}. Inset highlights the steric clash between the activation segment of NDR1 (purple) and the substrate elF2α bound to PKR (right inset). B. Superimposition of ROCK1-RhoE (PDB: 2V55; Komander et al., 2008) and NDR1^{KD}. Inset highlights the steric clash between the activation segment of NDR1 (purple) and the substrate RhoE (pink) bound to ROCK1. C. Superimposition of BRAF-MEK1 (PDB: 4MNE; Haling et al., 2014) and NDR1^{KD}. Inset highlights the steric clash between the activation segment of NDR1 (purple) and the substrate MEK1 (pink) bound to BRAF. (Supp. Figure 5 relates to Figure 3).

Supplementary Figure 6

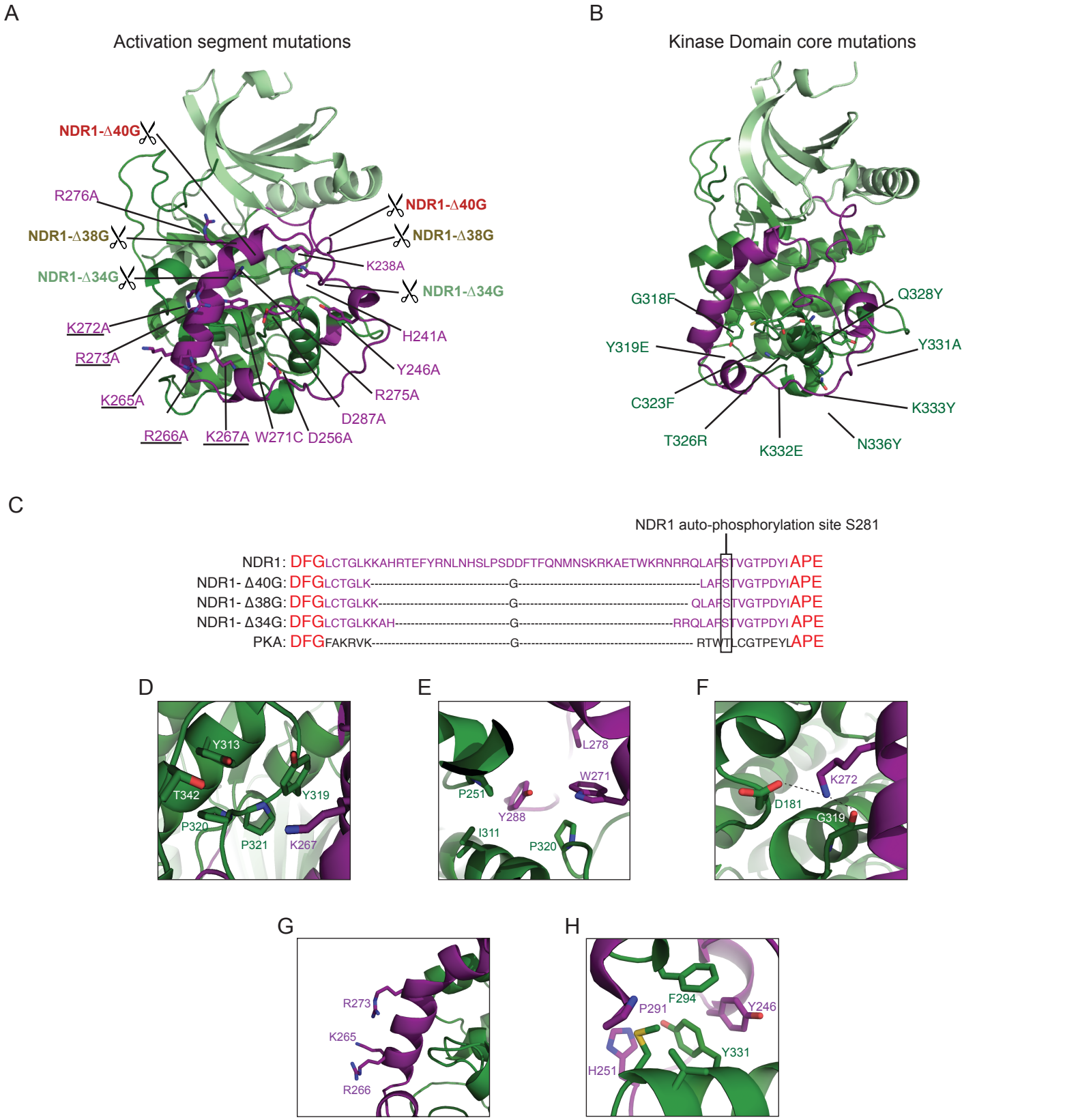

Supp. Figure 6. Mutational analysis of the activation segment of human NDR1. A. Ribbon diagram of NDR1^{KD} highlighting mutations generated and functionally characterized (see accompanying Figure 5) within the activation segment. B. Ribbon diagram of NDR1^{KD} highlighting mutations generated and functionally characterized on the kinase domain core. C. Sites of deletion mutations are highlighted by scissors and the sequences deleted. Panels D-H correspond to zoomed-in views relative to the structure shown in Figure 1B of the contact sites between the activation segment of NDR1 and the protein kinase core. Figures are colored as in Figure 1B. (Supp. Figure 6 relates to Figure 5).

Supplementary Figure 7

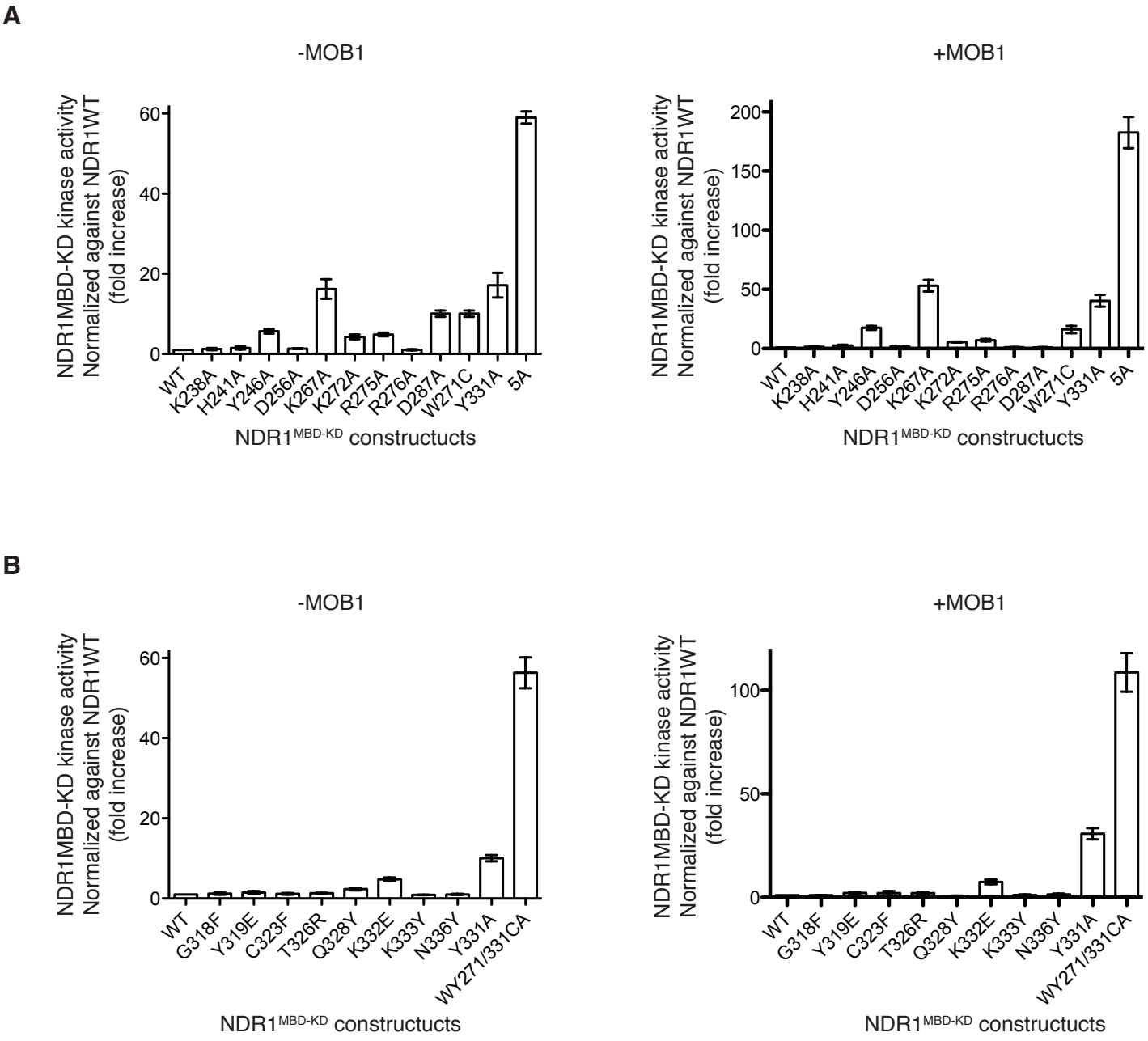

Supp. Figure 7. Quantification of RAB3IP phosphorylation by wild-type NDR1^{MBD-KD} and the indicated mutants in the absence and presence of MOB1. See Figure 5 for the corresponding kinase assays. n=3 experiments done in technical duplicate; error bars, SEM. (Supp. Figure 7 relates to Figure 5).

Supplementary Figure 8

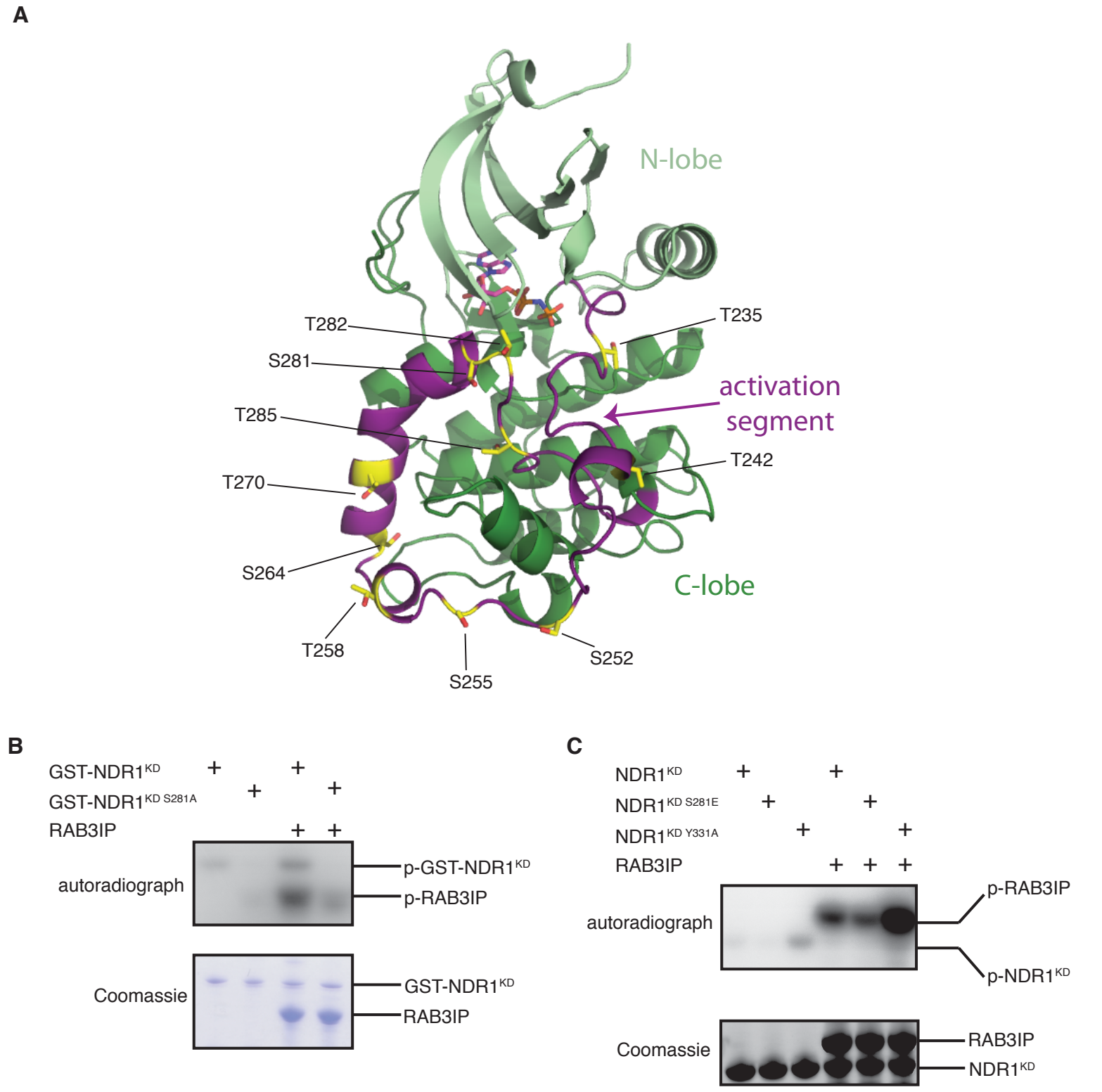

Supp. Figure 8. Effect of mutations to the Ser281 auto-phosphorylation site of NDR1 on in vitro kinase activity. A. Ribbon representation of the kinase domain of NDR1 highlighting the position of 10 serine and threonine residues with regulatory potential. B. In vitro analysis of auto-phosphorylation and the phosphorylation of RAB3IP substrate by wild-type NDR1^{KD} and the indicated S281A mutant. The top panel displays the autoradiograph, and the bottom panel shows protein loading by Coomassie staining. C. In-vitro analysis of auto-phosphorylation and the phosphorylation of RAB3IP substrate by wild-type NDR1^{KD} and the indicated S281E and Y331A mutants. The top panel displays the autoradiograph, and the bottom panel shows protein loading by Coomassie staining. (Supp. Figure 5 relates Figures 4 & 5).

Supplementary Figure 9

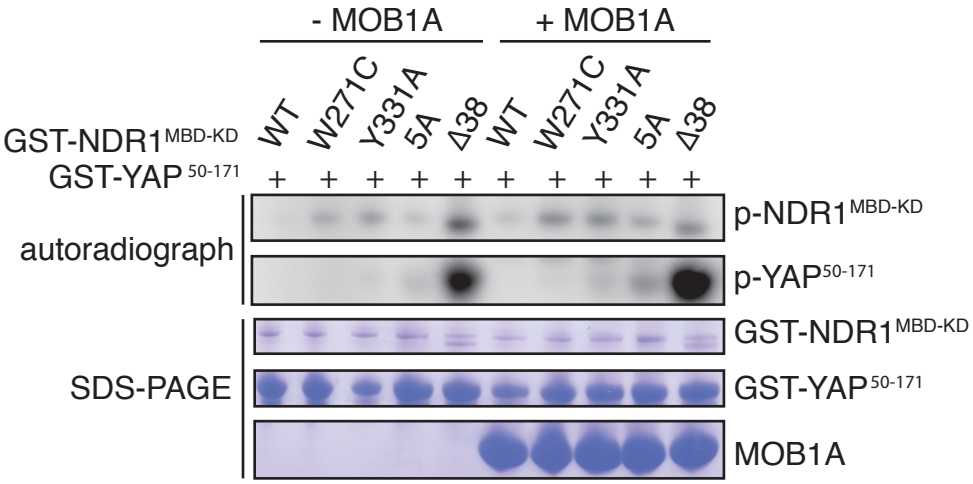

Supp. Figure 9. Mutational analysis of the activation segment of human NDR1. In vitro phosphorylation of the NDR1 substrate GST-YAP$^{50-171}$ by wild-type NDR1^{MBD-KD} and the indicated point mutants with or without the addition of MOB1A. (Supp. Figure 9 relates to Figure 5).